Journal of Hazardous Materials, 35 (1993) 31–51
Elsevier Science Publishers B.V., Amsterdam

A three-dimensional air flow model for soil venting: Superposition of analytical functions

Jong Soo Cho

U.S. EPA, Robert S. Kerr Environmental Research Laboratory, P.O. Box 1198, Ada, OK 74820 (USA)

(Received May 10, 1992; accepted in revised form March 6, 1993)

Abstract

A three-dimensional computer model was developed for the simulation of the soil-air pressure distribution at steady state and specific discharge vectors during soil venting with multiple wells in unsaturated soil. The Kirchhoff transformation of dependent variables and coordinate transforms allowed the adoption of the superposition of analytical functions to satisfy the differential equations and boundary conditions. A venting well was represented with a line source of a finite length in a infinite homogeneous medium. The boundary conditions at the soil surface and the water table were approximated by the superposition of a large number of mirror image wells on the opposite sides of boundaries. The numerical accuracy of the model was checked by the evaluation of one of the boundary conditions and the comparison of a simulation result with an available analytical solution from the literature. Simulations of various layouts of operating systems with multiple wells required minimal computational expenses. The model was very flexible and easy to use, and its numerical results proved to be sufficiently accurate.

Introduction

Leaks and spills are the major causes of soil and groundwater contamination in underground storage tank areas. In many cases, a large portion of the hydrocarbon remains in the unsaturated zone, forming a residual immiscible liquid which serves as a long-term source of groundwater contamination. Groundwater remediation should include the removal of the long-term sources. Soil venting, or vacuum extraction, has become a popular technology since it has been shown to be very effective for removing volatile organic compounds (VOCs) from the unsaturated soil. The principles of soil venting are very simple, but the complicated properties of soil and contaminants in the field have made the design of a soil venting system empirical and site-specific (Hutzler et al. [1]). In many cases, pilot-scale tests have been conducted on-site to obtain operational parameters for full scale systems (U.S. EPA [2]).

Mathematical models have been developed to study physical and chemical processes involved in soil venting and used to analyze laboratory and field-scale experiments. Analytical solutions of air pressure changes in one-dimensional porous media were obtained by Roberts [3] and Kidder [4]. McWhorter [5] developed a pseudo-analytical integral solution for the unsteady radial flow of gas in the unsaturated zone. Baehr and Hult [6] and Joss et al. [7] reported analytical solutions for air flow at steady state in radial and axial directions. Shan et al. [8] obtained analytical solutions of gas flow at steady state in an axisymmetric cylindrical domain and also presented test procedures to obtain soil-air permeability. Wilson et al. [9] developed a model and analyzed soil column experiments conducted by the AWARE, Inc. [10]. Wilson et al. [11] developed a model to simulate sand box experiments of the Texas Research Institute (Wootan and Voynick [12]). Falta et al. [13] and Mendoza and Frind [14] studied density-driven air flow in the unsaturated zone with models. Baehr et al. [15] reported laboratory soil column experiments and model development. Rathfelder et al. [16] developed a two-dimensional model to study chemical, field, and system variables which affect the removal of contaminants by soil venting.

Computer models have been used as an aid in designing field systems. Models have been developed to design methane gas control systems in landfills (Moore et al. [17], Mohsen et al. [18], Moore et al. [19], Metcalf and Farquhar [20], Young [21]), and soil venting systems for remediation of VOC contaminated soil (Sabadell et al. [22], Johnson et al. [23], Walton et al. [24]). The physical similarity between groundwater pumping and vacuum extraction of soil air led to the use of groundwater models for the design of soil venting. Massmann [25] suggested that a groundwater flow model would be a good tool in the simulation of air flow. An application of a three-dimensional USGS groundwater flow model for the simulation of air flow during soil venting was reported by Cho and DiGiulio [26].

Most numerical models use either the finite difference or finite element method for multidimensional simulations, which require a large amount of computer memory and computational time. Analytical solution models are limited to very simple situations such as a single well operation in homogeneous media. Since the effective zone of a single venting well does not cover the whole contaminated area, multiple wells are installed to increase the effective zone of soil venting. Soil-air movement and pressure propagation become three-dimensional in space, and can be described with partial differential equations and several boundary conditions. Generally, numerical methods are used to obtain solutions by approximating either the differential equations or the boundary conditions. The finite-difference and finite-element methods use the approximation to the differential equations. The superposition or integration of analytical functions which exactly satisfy the differential equations over the boundaries can be adopted to approximate the boundary conditions, which include the boundary integral method (Liggett and Liu [27]) and the analytical element method (Strack [28]). These methods eliminate mesh generation inside the solution domain, and only the boundary conditions should be approximated. Therefore, these methods require a small amount of computational time when the boundary conditions are not complicated (Hess and Smith [29]). Irregular shapes or heterogeneous property distributions inside the solution domain generate complicated conditions which should be satisfied. Under these conditions, both the finite difference method and finite element method are superior to the boundary approximation method. Therefore, the use of boundary approximation methods has been restricted to domains with limited heterogeneity.

During soil venting operations in the unsaturated soil, the pressure distribution arrives at steady state in a short time (several hours or days), except in a very low permeability soil, like clay, where it may take several weeks or even months. It may be reasonable to use the steady state solutions of air flow during soil venting, an operation which usually continues over several months. It is also assumed that thermodynamic and transport properties of soil air do not change much due to evaporation of VOCs. Therefore, soil-air flow can be solved separately from chemical transport equations. In this paper, the mathematical development of a three-dimensional soil-air flow model for soil venting is described. The model described in this paper simulates only the convective air flow during soil venting and does not include the chemical transport processes which are germane to soil venting. A simple transformation of the dependent variable and coordinate in the mass balance equation of soil-air at steady state yields the classical Laplace equation, whose analytical solutions can be easily obtainable from potential theory (Wilson et al. [9], Shan et al. [8]). Wilson et al. [9] considered the venting well as a point source of the fluid potential and used the mirror image method to satisfy the boundary conditions. Shan et al. [8] treated a venting well as a line source and obtained the line source solution by integrating the point solution of Wilson et al. [9] along the well axis. Since both solutions were based on the axisymmetric cylindrical coordinate system, only a single well operation could be simulated. In this paper, a three-dimensional rectangular coordinate system is adopted, and solutions are obtained for multiple well operations. A numerical accuracy analysis of the model and example simulations are also presented in this paper.

Model development

Air flow in soil

The mass conservation of air in the unsaturated soil is expressed by

$$\phi\frac{\partial\rho}{\partial t}=-\nabla(\rho \boldsymbol{V}) \tag{1}$$

where ϕ is the air filled porosity, ρ is the soil-air density, $\boldsymbol{V}$ is the specific discharge (vector), and t is the time.

Darcy's law applied to air flow in porous media is

$$V = -\frac{\mathbf{k}\rho}{\mu} \cdot \nabla \Phi \tag{2}$$

where Φ is the flow potential, $\mathbf{k}$ is the soil-air permeability tensor, and μ is the soil-air viscosity.

The flow potential is defined for the compressible fluid as

$$\Phi = gz + \int_{P_o}^{P} \frac{\mathrm{d}P}{\rho} \tag{3}$$

where g is the gravity constant, P is the pressure, z is the elevation, and P_o is the pressure at reference state.

The air density is a function of pressure and is expressed by the ideal gas law.

$$\rho = \mathrm{M}P/RT \tag{4}$$

where M denotes the average molecular weight of soil-air, R the ideal gas-law constant, and T the absolute temperature of soil-air.

Equations (3) and (4) generate an expression for the flow potential as a function of pressure

$$\Phi = gz + \frac{RT}{\mathrm{M}} \ln \frac{P}{P_o} \tag{5}$$

Then, the flow potential gradient becomes

$$\nabla\Phi = g\nabla z + \frac{RT}{P\mathrm{M}} \nabla P \tag{6}$$

Since the effect of gravity on air movement in the unsaturated soil is negligible under highly convective conditions such as those existing during soil venting, the specific discharge vector can be expressed as

$$V = -\frac{\mathbf{k}}{\mu} \cdot \nabla P \tag{7}$$

Substitution of the specific discharge term with eq. (7) into the mass conservation equation (1) yields the following equation for soil-air pressure

$$\phi \frac{\partial}{\partial t}\left(\frac{\mathrm{M}P}{RT}\right) = \nabla \cdot \left(\frac{\mathrm{M}P}{RT} \frac{\mathbf{k}}{\mu} \cdot \nabla P\right) \tag{8}$$

Assuming that temperature, molecular weight, viscosity, and soil-air permeabilities are constant during the operation period and uniform in the operating zone, the mass conservation equation can be simplified as

$$\phi \frac{\partial P}{\partial t} = \frac{\mathbf{k}}{\mu} \cdot \nabla \cdot (P \nabla P) \tag{9}$$

At steady state, eq. (9) becomes

$$\nabla\cdot(P\nabla P)=0 \tag{10}$$

The Kirchhoff transform of P as

$$\frac{\mathrm{d}m}{\mathrm{d}P}=2P \tag{11}$$

or

$$m=P^2-P_a^2 \tag{12}$$

where P_a is the atmospheric pressure, converts eq. (10) to a Laplace equation

$$\nabla^2 m=0 \tag{13}$$

The Laplace equation is a common expression for steady state fluid potential distribution in hydrodynamics. The following four boundary conditions can be applied for soil venting in the unsaturated soil (Fig. 1).

(1) At slotted sections of venting wells, a constant pressure can be assigned

$$P_{\text{slotted well surface}}=P_w \tag{14}$$

which becomes

$$m_{\text{slotted well surface}}=P_w^2 \tag{15}$$

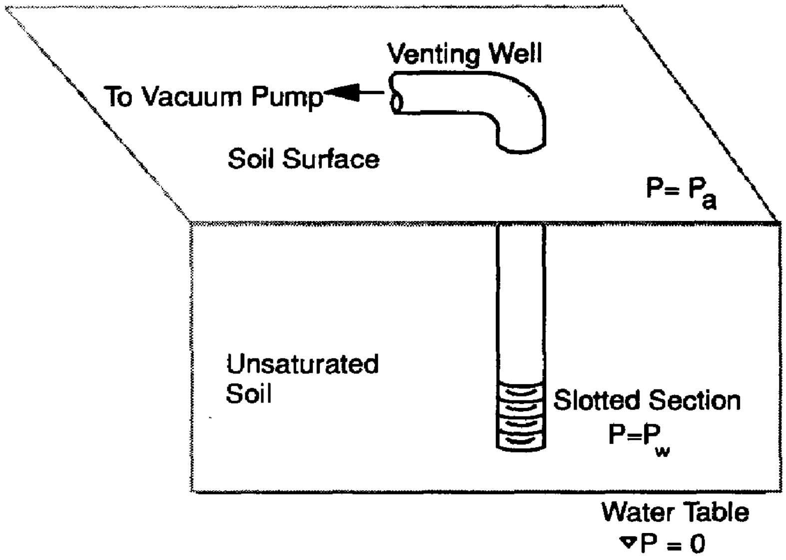

Fig. 1. A schematic diagram of soil venting system.

(2) At the boundaries with specified values of pressures; i.e., the soil surface exposed to the atmosphere

$$P_{\text{soil surface}} = P_a \tag{16}$$

which can be expressed

$$m_{\text{soil surface}} = 0 \tag{17}$$

(3) At the boundaries with specified flux conditions; i.e., the water table and fully covered soil surface, where no flux conditions are assigned

$$\nabla P_{\text{water table}} = 0 \tag{18}$$

which is

$$\nabla m_{\text{water table}} = 0 \tag{19}$$

(4) Finally, at remote locations from the operating zone with constant soil-air

$$P_\infty = P_a \tag{20}$$

which is

$$m_\infty = 0 \tag{21}$$

Solutions for homogeneous isotropic soil

A solution to the Laplace equation (13) due to a point source in an infinite domain is

$$m = -\frac{q}{4\pi} \times \frac{1}{s} \tag{22}$$

where s is the distance from the point source and q is the specific strength of the point source. The slotted section on the soil venting well can be interpreted as a finite length line source (Fig. 2) located at the well axis. Assuming a uniform distribution of the source strength along the source line, the solution to the Laplace equation (13) due to a line source (Haitjema [30]) becomes

$$m = -\frac{Q}{4\pi} \ln \frac{u+v-2h}{u+v+2h} \tag{23}$$

where u, v, and h are the lengths of vectors defined in Fig. 2. The unknown value of the source strength, Q, should be determined by satisfying the first boundary condition on the slotted section of the venting well (eq. 15). In a rectangular Cartesian coordinate system, u, v, and h are expressed as

$$u = \sqrt{(x-x_t)^2 + (y-y_t)^2 + (z-z_t)^2} \tag{24}$$

$$v = \sqrt{(x-x_b)^2 + (y-y_b)^2 + (z-z_b)^2} \tag{25}$$

$$h = \tfrac{1}{2}\sqrt{(x_t-x_b)^2 + (y_t-y_b)^2 + (z_t-z_b)^2} \tag{26}$$

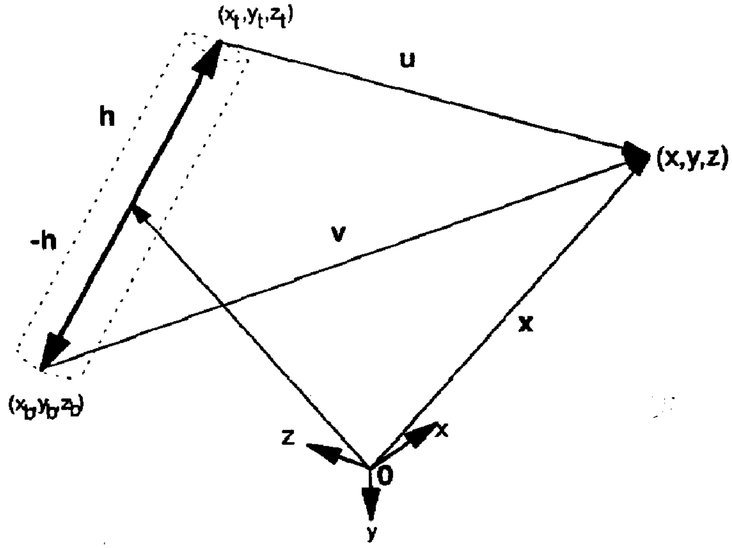

Fig. 2. Representation of soil venting well as a line source in rectangular coordinates.

The second and third boundary conditions (eqs. 17 and 19, respectively) can be satisfied by locating mirror image wells at the opposite side of the boundaries. By assigning an equal but negative value of the source strength on the mirror image well, zero potential at the boundary can be satisfied (Fig. 3). With an equal value of strength on the mirror image well, the third boundary condition of no flux can be satisfied (Fig. 4). If two boundaries like the soil surface and the water table exist and are parallel to each other, boundary conditions on both boundaries should be satisfied by locating an infinite number of mirror image wells on both sides of boundaries (Ferris et al. [31]) and summing all the values of m due to wells (Fig. 5). The solution of m in the domain becomes

$$m=-\frac{Q}{4\pi}\ln\frac{u+v-2h}{u+v+2h}+\sum_{i=1}^{\infty}-\frac{Q_i}{4\pi}\ln\frac{u_i+v_i-2h_i}{u_i+v_i+2h_i} \tag{27}$$

The analytical solution of m (eq. 27) exactly satisfies the Laplace equation and all the boundary conditions except at source locations where it has singularities. The solution of m due to N operating wells can be obtained as

$$m=\sum_{j=1}^{N}m_j \tag{28}$$

The pressure distribution can be obtained as

$$P=\sqrt{m+P_a^2} \tag{29}$$

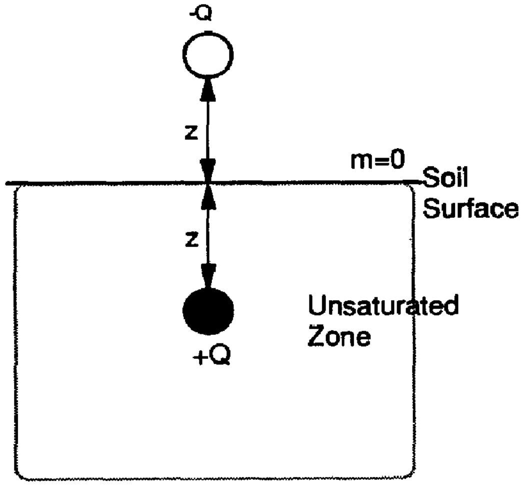

Fig. 3. Location of image well at constant pressure boundary.

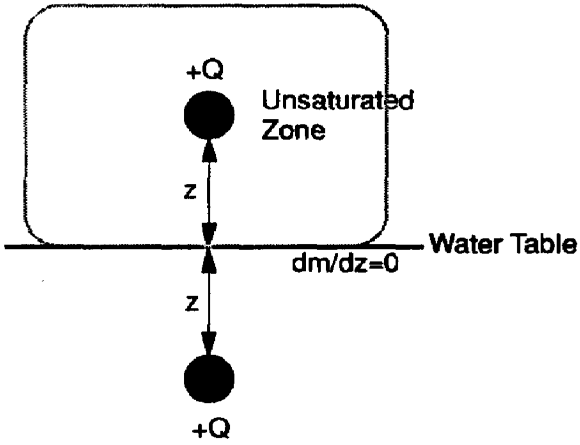

Fig. 4. Location of image well at zero flux boundary.

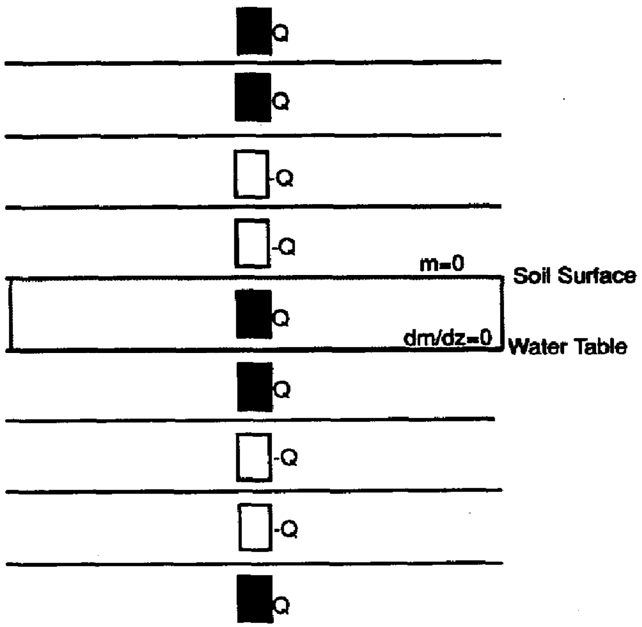

Fig. 5. An infinite number of image wells for two parallel boundaries.

and the specific discharge vector is

$$V = -\frac{\mathbf{k}}{\mu}\cdot\nabla P = -\frac{\mathbf{k}}{\mu}\cdot\frac{\nabla m}{2P} \tag{30}$$

When the coordinate axes coincide with the principal axes of the permeability tensor in the rectangular coordinate, and $k = k_x = k_y = k_z$, the specific discharge in the x direction, V_x, can be obtained

$$V_x = -\frac{k}{\mu}\frac{1}{2\sqrt{m+P_a^2}}\sum_{j=1}^{N}\frac{\partial m_j}{\partial x} \tag{31}$$

where

$$\frac{\partial m_j}{\partial x} = -\frac{Q}{\pi}\frac{h\left(\dfrac{x-x_t}{u}+\dfrac{x-x_b}{v}\right)}{(u+v+2h)(u+v-2h)} + \sum_{i=1}^{\infty}\frac{-Q_i}{\pi}\frac{h_i\left(\dfrac{x-x_{it}}{u_i}+\dfrac{x-x_{ib}}{v_i}\right)}{(u_i+v_i+2h_i)(u_i+v_i-2h_i)} \tag{32}$$

V_y is given by

$$V_y = -\frac{k}{\mu}\frac{1}{2\sqrt{m+P_a^2}}\sum_{j=1}^{N}\frac{\partial m_j}{\partial y} \tag{33}$$

where

$$\frac{\partial m_j}{\partial y} = -\frac{Q}{\pi}\frac{h\left(\dfrac{y-y_t}{u}+\dfrac{y-y_b}{v}\right)}{(u+v+2h)(u+v-2h)} + \sum_{j=1}^{\infty}\frac{-Q_i}{\pi}\frac{h_i\left(\dfrac{y-y_{it}}{u_i}+\dfrac{y-y_{ib}}{v_i}\right)}{(u_i+v_i+2h_i)(u_i+v_i-2h_i)} \tag{34}$$

V_z becomes

$$V_z = -\frac{k}{\mu}\frac{1}{2\sqrt{m+P_a^2}}\sum_{j=1}^{N}\frac{\partial m_j}{\partial z} \tag{35}$$

where

$$\frac{\partial m_j}{\partial z} = -\frac{Q}{\pi}\frac{h\left(\dfrac{z-z_t}{u}+\dfrac{z-z_b}{v}\right)}{(u+v+2h)(u+v-2h)} + \sum_{i=1}^{\infty}\frac{-Q_i}{\pi}\frac{h_i\left(\dfrac{z-z_{it}}{u_i}+\dfrac{z-z_{ib}}{v_i}\right)}{(u_i+v_i+2h_i)(u_i+v_i-2h_i)} \tag{36}$$

Anisotropic media

In a homogeneous soil with anisotropic permeabilities, k_x, k_y, and k_z in x, y, z directions, the following Laplace equation can be derived by simple coordinate transformation of eq. (9)

$$\frac{\partial^2 m}{\partial x^{*2}}+\frac{\partial^2 m}{\partial y^{*2}}+\frac{\partial^2 m}{\partial z^{*2}}=0 \tag{37}$$

where

$$x^* = x \tag{38}$$

$$y^* = y\sqrt{k_x/k_y} \tag{39}$$

$$z^* = z\sqrt{k_x/k_z} \tag{40}$$

The anisotropic permeabilities are transformed into

$$k^* = k_x = k_y(\sqrt{k_x/k_y})^2 = k_z(\sqrt{k_x/k_z})^2 \tag{41}$$

The specific discharge vector can be obtained as

$$V_x = V_{x^*} \tag{42}$$

$$V_y = V_{y^*}\sqrt{k_x/k_y} \tag{43}$$

$$V_z = V_{z*}\sqrt{k_x/k_z} \tag{44}$$

where

$$V_{x^*} = -\frac{k^*}{\mu}\frac{1}{2\sqrt{m+P_\mathrm{a}^2}}\frac{\partial m}{\partial x^*} \tag{45}$$

$$V_{y^*} = -\frac{k^*}{\mu}\frac{1}{2\sqrt{m+P_\mathrm{a}^2}}\frac{\partial m}{\partial y^*} \tag{46}$$

$$V_{z*} = -\frac{k^*}{\mu}\frac{1}{2\sqrt{m+P_\mathrm{a}^2}}\frac{\partial m}{\partial z^*} \tag{47}$$

Cylindrical coordinate system

For a single well operation, a cylindrical coordinate system can be adopted, in which the well axis is located on the vertical axis of the coordinate, and a line source is assigned to the slotted section of the well (Fig. 6). Equations (24), (25), and (26) then become

$$u = \sqrt{r^2 + (z - z_\mathrm{t})^2} \tag{48}$$

$$v = \sqrt{r^2 + (z - z_\mathrm{b})^2} \tag{49}$$

$$h = \tfrac{1}{2}\sqrt{(z_\mathrm{t} - z_\mathrm{b})^2} \tag{50}$$

The radial discharge from the well can be obtained by differentiating the potential with respect to the radial coordinate

$$V_r = -\frac{k_r}{\mu}\frac{1}{2\sqrt{m+P_\mathrm{a}^2}}\frac{\partial m}{\partial r} \tag{51}$$

where

$$\frac{\partial m}{\partial r} = -\frac{Q}{\pi}\frac{h\left(\frac{r}{u}+\frac{r}{v}\right)}{(u+v+2h)(u+v-2h)} + \sum_{i=1}^{\infty}\frac{-Q_i}{\pi}\frac{h_i\left(\frac{r}{u_i}+\frac{r}{v_i}\right)}{(u_i+v_i+2h_i)(u_i+v_i-2h_i)} \tag{52}$$

and k_r is the soil-air permeability in radial direction. The vertical discharge, V_z, can be obtained as the eqs. (35) and (36). The flow into the well from

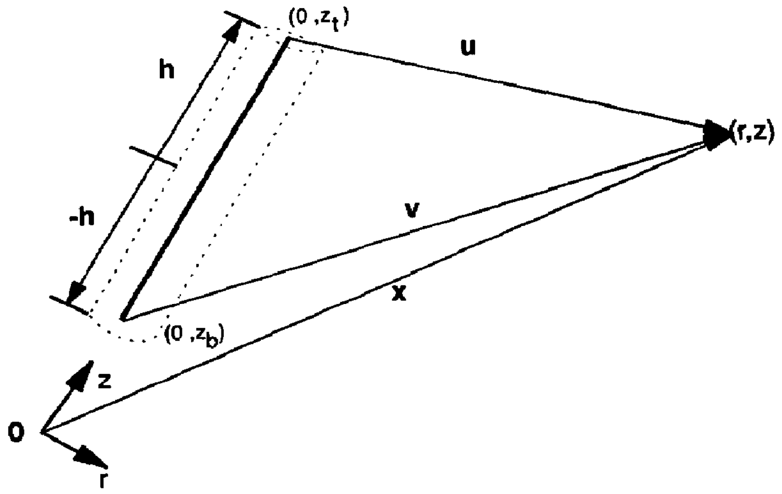

Fig. 6. Vector representation of a line source in cylindrical coordinates.

surrounding soil through the slotted section can be estimated by the integration of the radial discharge as

$$W|_{\text{well}} = -2\pi r_{\text{w}} \int_{z_b}^{z_t} V_r|_{r=r_{\text{w}}} \, \mathrm{d}z \tag{53}$$

where r_w is the radius of the well.

Numerical evaluation

Solutions of soil-air pressures and specific discharges were programmed with FORTRAN 77. In the current version of the model, the soil surface and water table were assumed to be parallel to each other and perpendicular to the vertical axis of the coordinate system. The evaluation of the model's numerical accuracy, by checking one boundary condition and comparing simulation results with an available analytical model in the open literature, is presented in this paper. Due to the computational limitations, a finite number of image wells had to be used instead of the infinite number of image wells. Semi-infinite line sources can be used to represent the infinite number of wells (cf. Haitjema [30], Wilson et al. [9], Shan et al. [8]). To evaluate errors associated with the finite number of image wells, the pressure distribution at the soil surface, which should satisfy the ambient conditions, was calculated with various numbers of image wells (simulation No. 1). Simulation conditions are listed in Table 1. Differences between the estimated pressure on the soil surface and the ambient pressure are plotted in Fig. 7. The errors become negligible as the number of imaginary well increases, and the number of image wells in the model could be limited to 400.

TABLE 1

Parameters used on simulations

Parameters	Simulation No.				
	1	2	3	4	5
Water table (m)	5	5	5	5	5
Number of wells	1	1	2	3	3
Well types	Extraction	Extraction	Extraction Injection	Injection Injection Extraction	Injection Injection Extraction
Well diameter (cm)	10	10	10 10	10 10 10	10 10 10
Length of slotted section (m)	1	1	1 1	1 1 10	1 1 10
Location of slotted section from water table (cm)	70	70	70 70	70 70 400	70 70 400
Well pressure (atm)	0.9	0.9	0.9 1.1	1.1 1.1 0.9	1.1 1.1 0.9
k_x (cm^2)	5.0×10^{-8}	5.0×10^{-8}	5.0×10^{-8}	5.0×10^{-8}	5.0×10^{-8}
k_y (cm^2)	5.0×10^{-8}	5.0×10^{-8}	5.0×10^{-8}	5.0×10^{-8}	5.0×10^{-8}
k_z (cm^2)	5.0×10^{-8}	5.0×10^{-9}	5.0×10^{-8}	5.0×10^{-8}	5.0×10^{-8}
Covered on soil surface	No	No	No	No	Yes

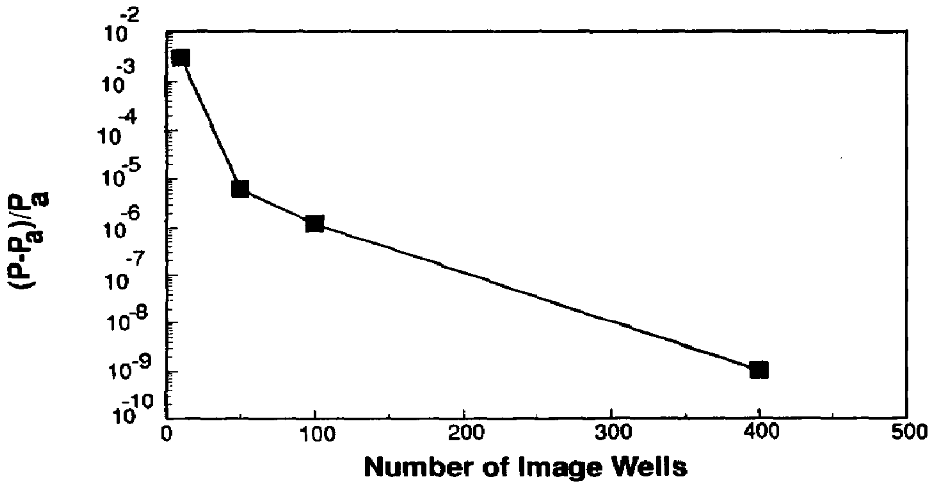

Fig. 7. Estimated error at soil surface with number of image wells.

Baehr and Hult [6] presented analytical solutions of the mass conservation equation (9) at steady state in the cylindrical coordinate system (Fig. 8). They used the Laplace transform with Fourier sine and cosine transforms to obtain analytical solutions. Their solutions were used with non-linear least-squares data fitting techniques to obtain soil-air permeabilities from pneumatic pumping tests (Baehr and Hult [6], Cho and DiGiulio [32]).

Figure 9 shows the comparison of pressure distributions at the depth of 4 m obtained from simulations of soil venting with the current model and the

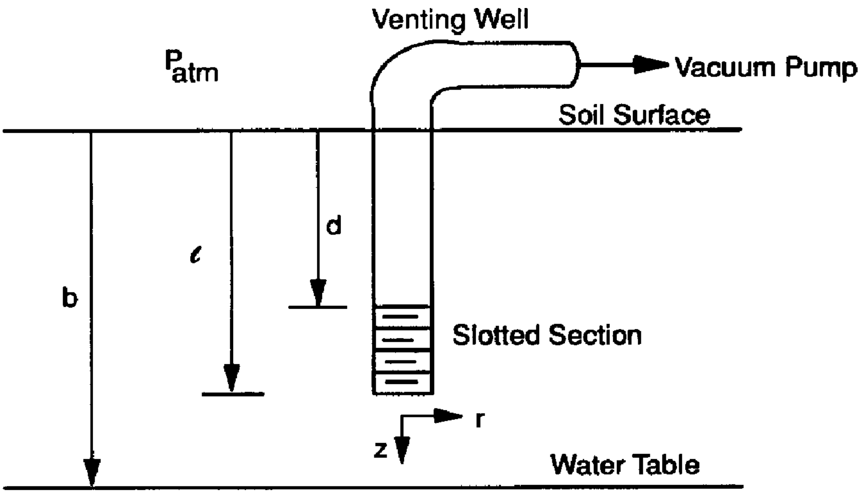

Fig. 8. A schematic diagram of Baehr and Hult's soil venting configuration.

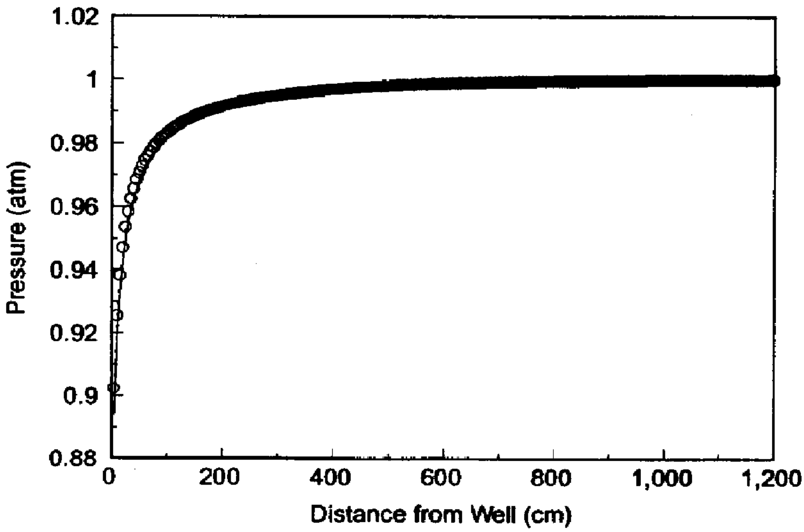

Fig. 9. Comparison of pressure distribution at 4 m below soil surface. (——) Baehr and Hult's solution, and (--○--) Current model.

analytical solution obtained by Baehr and Hult [6]. It shows close agreement between the two simulations.

Results of simulation studies

Simulations with various configurations were conducted and their results were evaluated to show the flexibility and computational efficiency of this model. A second simulation to evaluate anisotropic permeability effects on soil venting operations was conducted (simulation No. 2). Operating conditions were set identical to those of simulation No. 1, except that the permeability in the vertical direction was one-tenth of the horizontal permeability. The pressure distribution clearly shows that the low permeability in the vertical

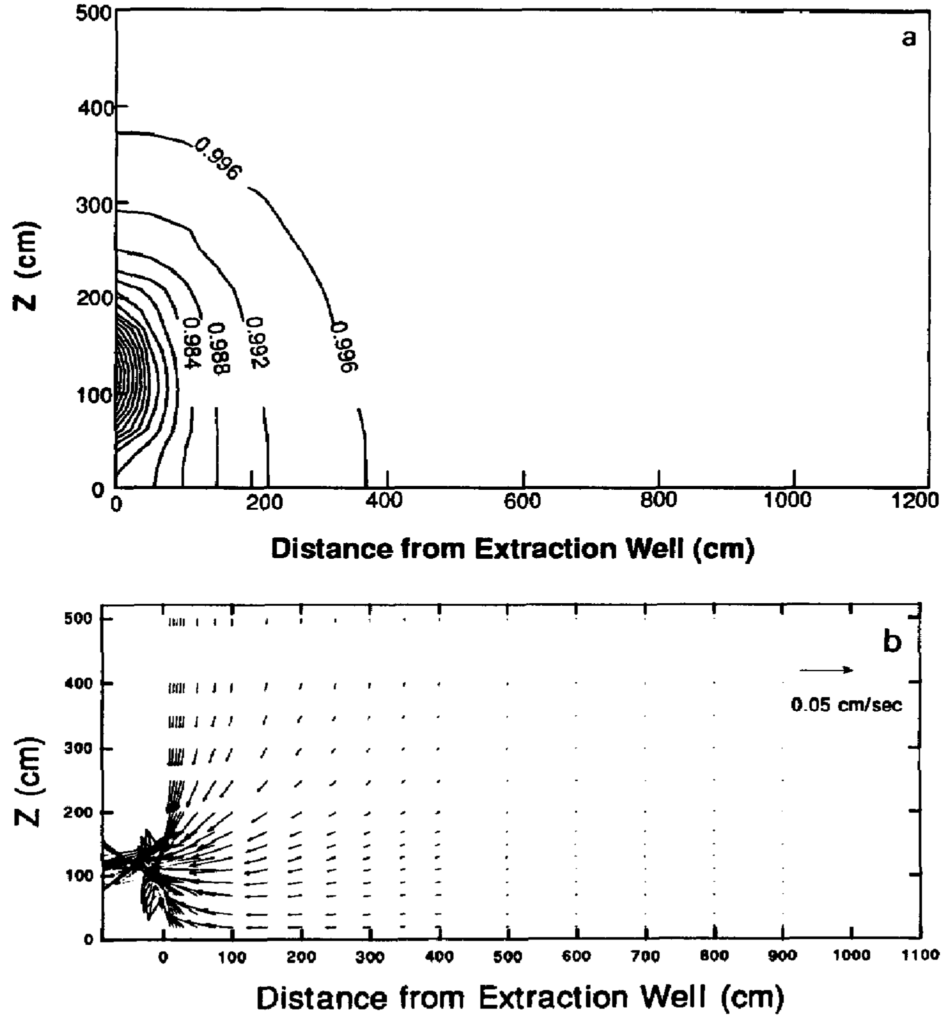

Fig. 10. (a) Soil-air pressure distribution for isotropic soil extraction well pressure at 0.9 atm. (b) Vector plot of specific discharge

direction increases the effective zone in the horizontal direction (Fig. 10 and 11). The vector plots of the specific discharge show more horizontal flow in the anisotropic medium than in the isotropic medium.

A third simulation was performed on the simultaneous operation of vacuum extraction and air injection wells (simulation No. 3). The location and operating conditions of the vacuum extraction well were identical to those of the first simulation. An air injection well was added at 12 m distance from the vacuum extraction well and its physical configurations were set identical to those of extraction wells. The injection air pressure was set to 1.1 atm. From plots of pressure distribution and specific discharge vectors (Fig. 12), it was found that the major flow area was limited to the proximity of the wells even though the injection well was used to increase the horizontal flow between two wells.

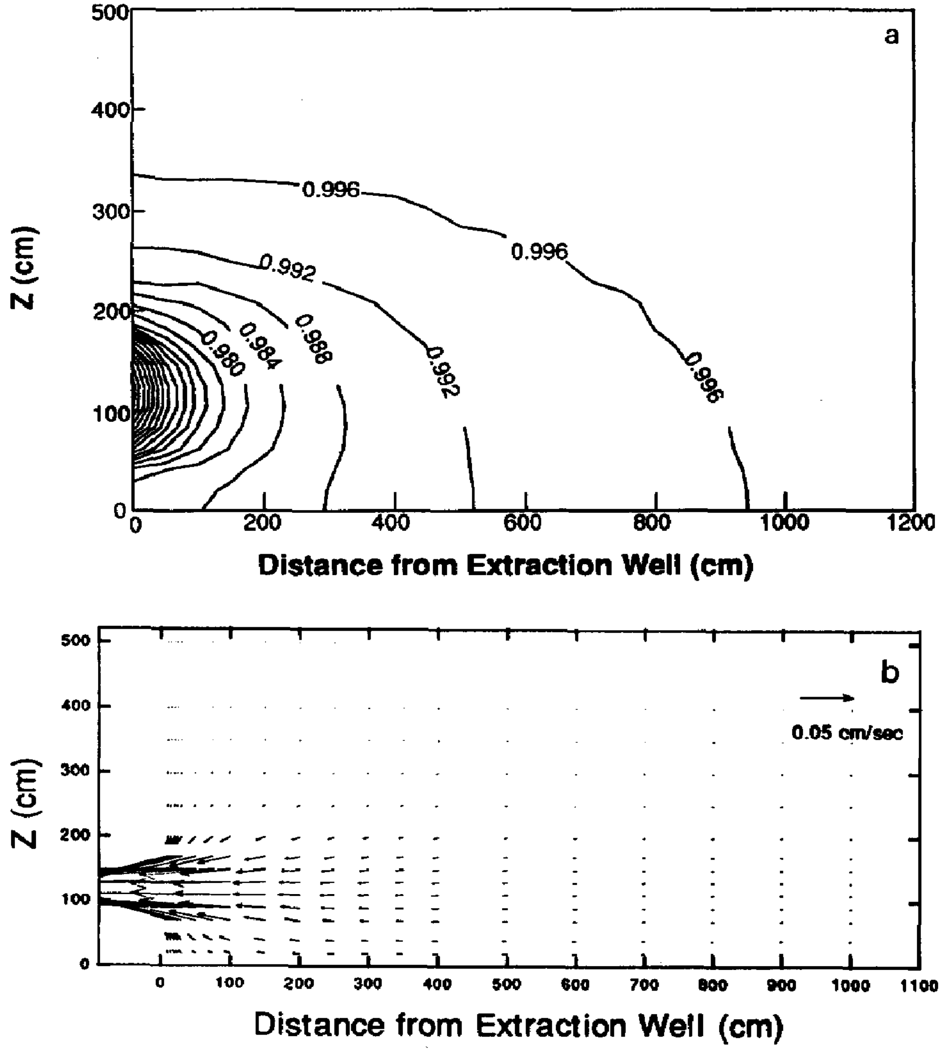

Fig. 11. (a) Soil-air pressure distribution for anisotropic soil extraction well pressure at 0.9 atm. (b) Vector plot of specific discharge.

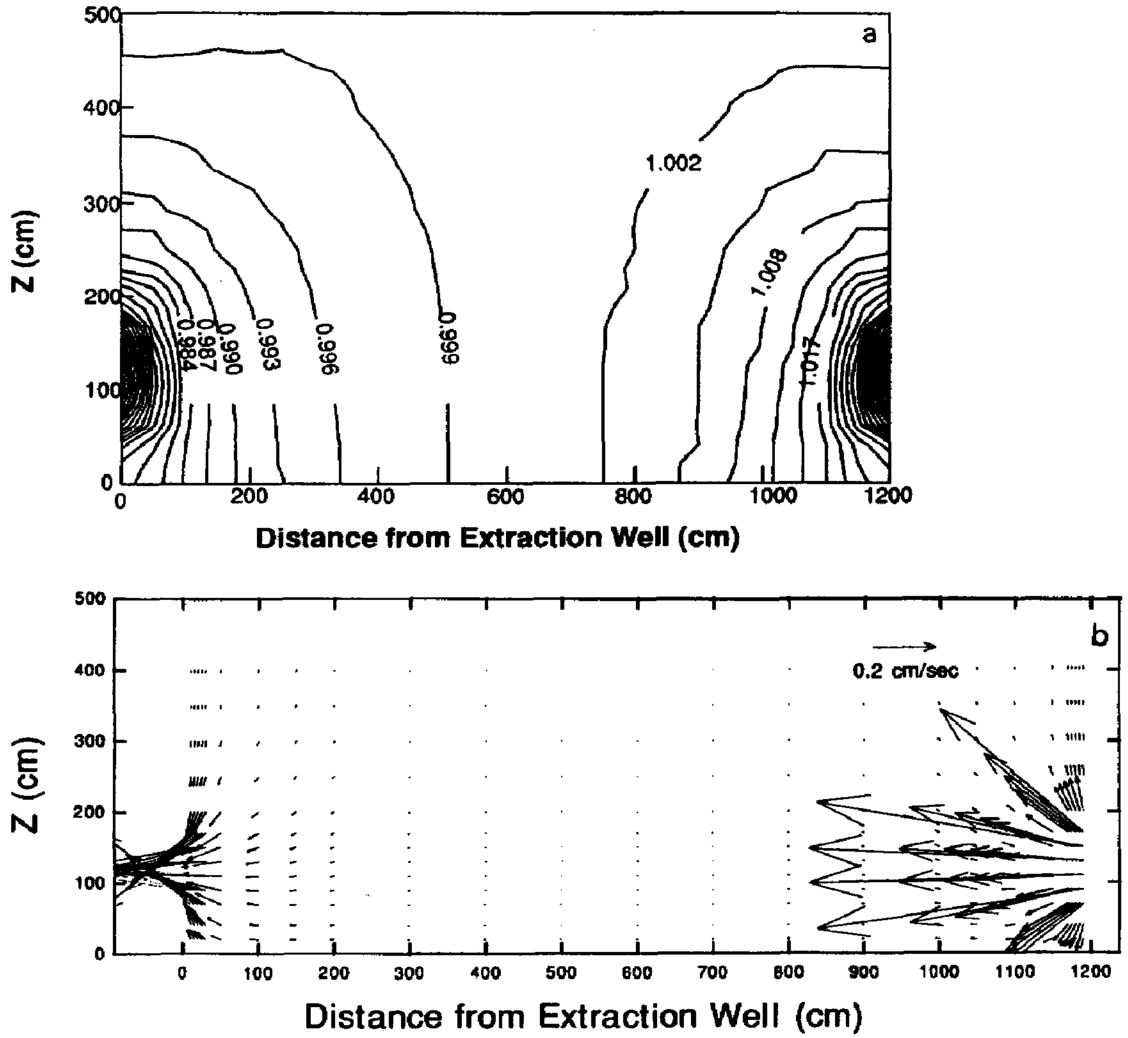

Fig. 12. Soil-air pressure distribution for injection/extraction operation extraction well pressure at 0.9 atm, injection well pressure at 1.1 atm. (b) Vector plot of specific discharge.

The next two simulations were on the combined operations of two vertical air injection wells and a horizontal extraction trench. The schematic diagram of the operating system is shown in Fig. 13. The effect of an impermeable layer on the soil surface, i.e. a plastic cover, was evaluated (simulation No. 4, Fig. 14) by comparison with the same type operation without a cover (simulation No. 5, Fig. 15). The covered soil surface increased the efficiency and the effective zone of the extraction trench by blocking the infiltration of the atmospheric air into the subsurface.

All the simulations were conducted with a personal computer. The number of computation points was about 250 for simulations of the single well operations and over 800 for the two vertical well and horizontal trench operations. Each computation used less than 60 seconds of CPU time on a 486 IBM PC. With

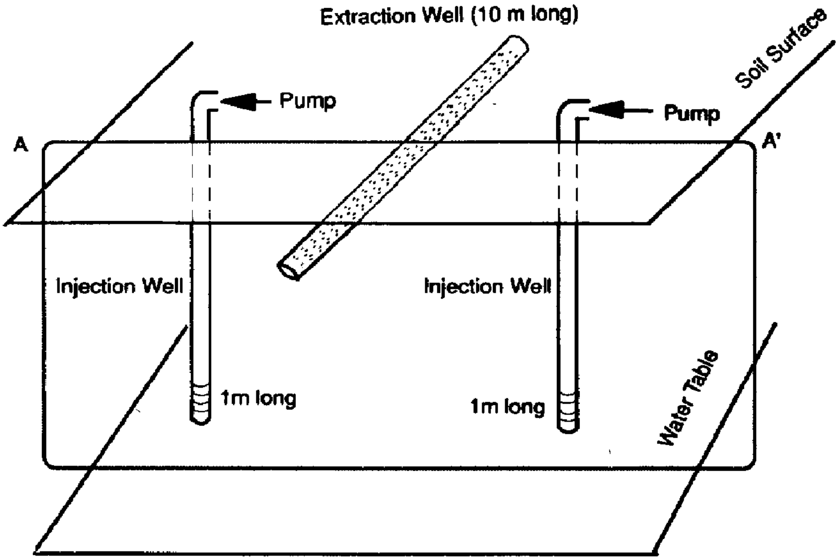

Fig. 13. A schematic diagram of two vertical wells and a horizontal well.

a simple preprocessor, it was not difficult to provide the input data file for simulations of the complicated layouts of operating conditions.

Summary and conclusions

In this paper, a semi-analytical model development for simulation of soil-air movement during soil venting in the unsaturated soil is presented. The summary and conclusions on the model are presented as follows:

(1) Assumptions in the model included the steady state on soil-air movement during soil-venting, constant properties of soil and soil-air, ideal gas on soil-air, and Darcy's law for soil-air movement.

(2) The mathematical applications included the Kirchhoff transforms of dependent variables, coordinate transformations, conversion of the soil-air conservation equation into a Laplace equation, and superpositions of analytical solutions of the Laplace equation for the partial differential equations and boundary conditions.

(3) Numerical accuracy was evaluated by checking boundary values and comparing soil-air pressure distribution with an available analytical solution in the literature. The model was found to be reasonably accurate.

(4) The flexibility and capability of handling complicated layouts of multiple wells in fully three-dimensional domains were tested through numerical simulations under various hypothetical conditions. The simulations show the model's capabilities of simulations without high computational expenses. Computations of soil-air pressures and discharge vectors required a minimal amount of computation time. The model seems to be suitable for personal computer applications.

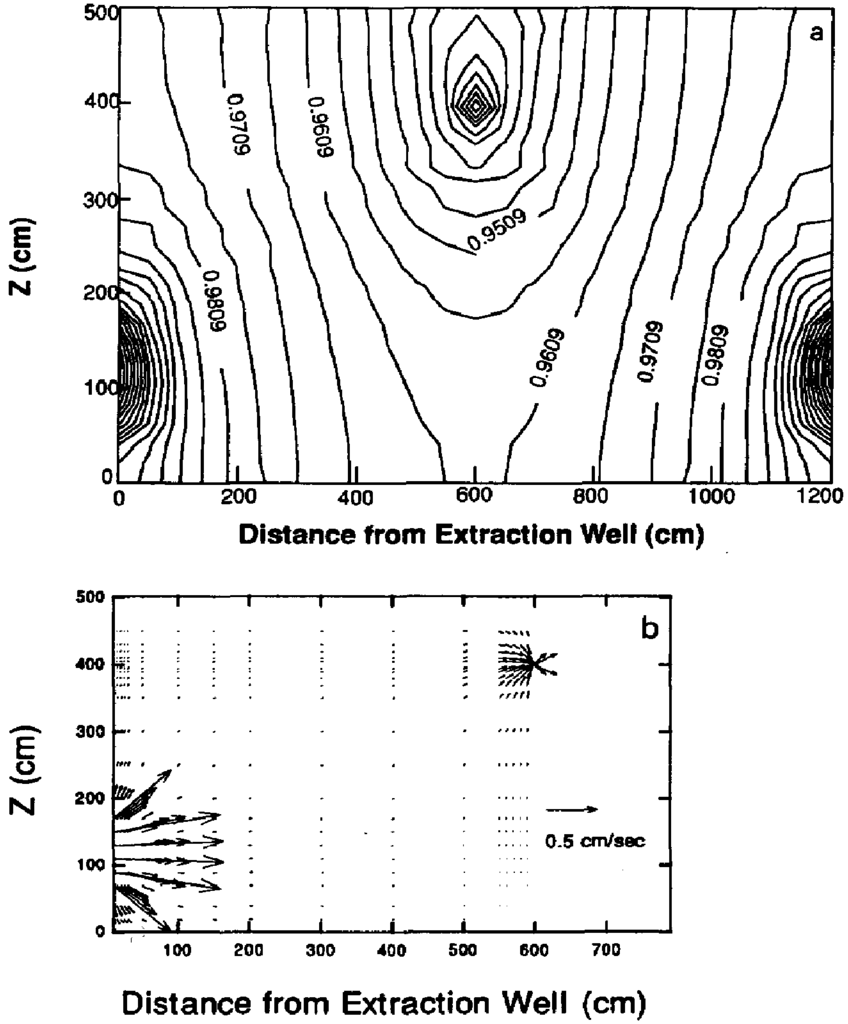

Fig. 14. (a) Soil-air pressure distribution for injection/extraction operation extraction wells at 0.9 atm, injection at 1.1 atm, covered soil surface. (b) Vector plot of specific discharge.

(5) The application of the current model is limited to computations of soil-air flow at steady state in homogeneous media because of the assumptions and mathematical methods. The limited heterogeneity will be handled by addition of analytical functions, e.g. point dipoles and line dipoles, on boundaries of heterogeneous regions to satisfy the conditions. Computed output of this model, e.g. specific discharge vectors, can be directed into other models which solve chemical transport equations by a finite difference or finite element method. The major contribution of this model development will be the derivations of analytical expressions which can be easily adopted in three-dimensional domains without a large computational expense.

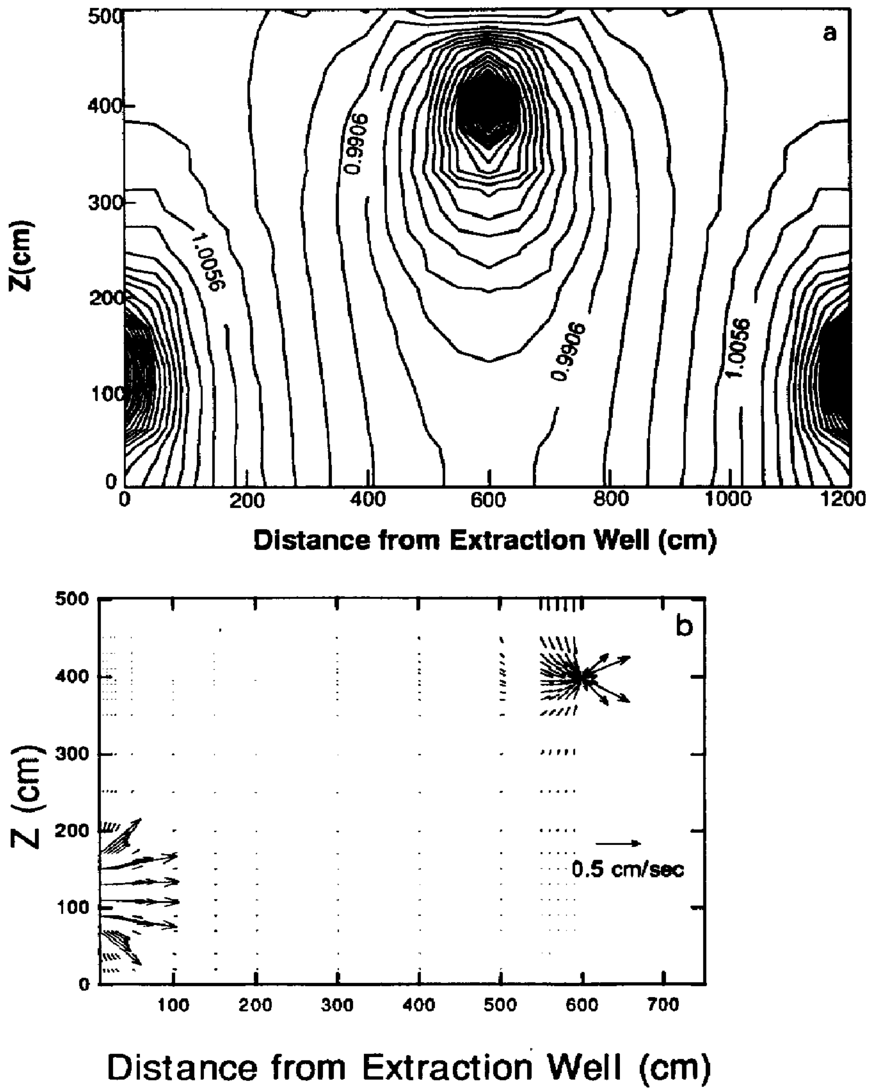

Fig. 15. (a) Soil-air pressure distribution for injection/extraction operation extraction wells at 0.9 atm, injection at 1.1 atm, uncovered soil surface. (b) Vector plot of specific discharge.

Acknowledgements

Although the research described in this article has been supported by the United States Environmental Protection Agency, it has not been subjected to the Agency review and therefore does not necessarily reflect the views of the Agency. The mention of trade names or commercial products does not constitute endorsement or recommendation for use. The author is deeply grateful to the three anonymous reviewers who helped improve the quality of the manuscript.

References

1 N.J. Hutzler, B.E. Murphy and J.S. Gierke, State of Technology Review, Soil Vacuum Extraction Systems, Final Report to U.S. EPA, CR-814319-01-1, Hazardous Waste Engineering Research Laboratory, Cincinnati, OH, 1988.
2 U.S. Environmental Protection Agency, Soil Vapor Extraction Technology — Reference Handbook, EPA/540/2- 91/003, U.S. EPA, Office of Research and Development, Washington, DC, 1991.
3 R.C. Roberts, Unsteady flow of a gas through a porous medium, In: Proc. of the First U.S. National Congress of Applied Mechanics, John Edward Inc., Ann Arbor, MI, 1951.
4 R.E. Kidder, Unsteady flow of gas through a semi-infinite porous medium, Trans. ASME, J. Appl. Mech., 24(3) (1957) 329–332.
5 D.B. McWhorter, Unsteady radial flow of gas in the vadose zone, J. Contaminant Hydrol., 5 (1990) 297–314.
6 A.L. Baehr and M.F. Hult, Evaluation of unsaturated zone air-permeability through pneumatic tests, Water Resour. Res., 27(10) (1991) 2605–2617.
7 C.J. Joss, A.L. Baehr and J.M. Fischer, A field technique for determining unsaturated zone air permeability, In: Proc. of Soil Venting Workshop, EPA/600/R-92/174, U.S. EPA, Robert S. Kerr Environmental Research Laboratory, Houston, TX, 1991, pp. 149–170.
8 C. Shan, R.W. Falta and I. Javandel, Analytical solutions for steady state gas flow to a soil vapor extraction well, Water Resour. Res., 28(4) (1992) 1105–1120.
9 D.J. Wilson, A.N. Clarke and J.H. Clarke, Soil cleanup by *in situ* aeration. I. Mathematical modeling, Sep. Sci. Technol., 23(10/11) (1988) 991–1037.
10 AWARE, Inc., Phase I, Zone 1 Soil Decontamination Through In-situ Vapor Stripping Processes, Final Report to U.S. EPA, Small Business Innovative Research Program, Contract No. 68-02-4446, Washington, DC, 1987.
11 D.E. Wilson, R.E. Montgomery and M.R. Sheller, A mathematical model for removing volatile subsurface hydrocarbons by miscible displacement, Water Air Soil Pollut., 33 (1987) 231–255.
12 W.L. Wootan and T. Voynick, Forced Venting to Remove Gasoline Vapor from a Large-Scale Model Aquifer, Texas Research Institute Final Report to American Petroleum Institute, Washington, DC, 1984.
13 R.W. Falta, I. Javandel, K. Pruess and P.A. Witherspoon, Density-driven flow of gas in the unsaturated zone due to the evaporation of volatile organic compounds, Water Resour. Res., 25(10) (1989) 2159–2169.
14 C.A. Mendoza and E.O. Frind, Advective-dispersive transport of dense organic vapors in the unsaturated zone, 1. Model development, Water Resour. Res., 26(3) (1990) 379–387.
15 A.L. Baehr, G.E. Hoag and M.C. Marley, Removing volatile contaminants from the unsaturated zone by inducing advective air-phase transport, J. Contaminant Hydrol., 4 (1989) 1–26.
16 K. Rathfelder, W.W. Yeh and D. Mackay, Mathematical simulation of soil vapor extraction systems: Model development and numerical examples, J. Contaminant Hydrol., 8 (1991) 263–297.
17 C.A. Moore, I.S. Rai and A.A. Alzaydi, Methane migration around sanitary landfills, ASCE J. Geotech. Eng. Div., 105(GT2) (1979) 131–144.
18 M.F.N. Mohsen, G.J. Farquhar and N. Kouwen, Gas migration and vent design at landfill sites, Water Air Soil Pollut., 13 (1980) 79–97.
19 C.A. Moore, I.S. Rai and J. Lynch, Computer design of landfill methane migration control, ASCE J. Environ. Eng. Div., 108(EE1) (1982) 89–106.
20 D.E. Metcalf and G.J. Farquhar, Modeling gas migration through unsaturated soils from waste disposal sites, Water Air Soil Pollut., 32 (1987) 247–259.
21 A. Young, Mathematical modeling of landfill gas extraction, ASCE J. Environ. Eng., 115(6) (1989) 1073–1087.

22 G.P. Sabadell, J.J. Eisenbeis and D.K. Sunada, The 3-D model CSUGAS; A management tool for the design and operation of soil venting system, In: Proc. of HMCRI's 9th Natl. Conf. and Exhib., Superfund '88, HMCRI Washington, DC, 1988, pp. 177–182.
23 P.C. Johnson, M.W. Kembloski and J.D. Colthart, Quantitative analysis for the cleanup of hydrocarbon-contaminated soils by in-situ soil venting, Ground Water, 28(3) (1990) 413–429.
24 J.C. Walton, R.G. Baca, J.B. Sisson, A.J. Sondrup and S.O. Magnuson, Applying computer simulation models to design large-scale soil venting and bioremediation systems, In: Proc. of Soil Venting Workshop, EPA/600/R- 92/174, U.S. EPA, Robert S. Kerr Environmental Research Laboratory, Houston, TX, 1991.
25 J.W. Massmann, Applying groundwater flow models in vapor extraction system design, ASCE J. Environ. Eng., 115(1) (1989) 129–149.
26 J. S. Cho and D.C. DiGiulio, The simulation of air flow in soil vacuum extraction systems by a 3-D groundwater flow model, In: Proc. of the Conf. on Hazardous Waste Research, Kansas State University, Manhattan, KS, 1990, pp. 621–635.
27 J.A. Liggett and P.L.-F. Liu, The Boundary Integral Equation Method for Porous Media Flow, George Allen and Unwin, London, UK, 1983.
28 O.D.L. Strack, Groundwater Mechanics, Prentice-Hall, Englewood Cliffs, NJ, 1989.
29 J.C. Hess and A.M.O. Smith, Calculation of Potential Flow About Arbitrary Bodies, Progress in Aeronautical Sciences, Vol. 8, Pergamon, New York, NY, 1967.
30 H.M. Haitjema, Modeling Three-Dimensional Flow in Confined Aquifers by Superposition of Both Two- and Three-Dimensional Analytic Functions, Water Resour. Res., 21(10) (1985) 1557–1566.
31 J.G. Ferris, D.B. Knowles, R.H. Brown and R.W. Stallman, Theory of Aquifer Tests, Geological Survey Water-Supply Paper 1536-E, U.S. Department of the Interior, Washington, DC, 1962.
32 J.S. Cho and D.C. DiGiulio, Pneumatic pumping test for soil vacuum extraction, Environ. Prog., 11(3), (1992) 228–233.